EEET ECOLOGICAL ENGINEERING & ENVIRONMENTAL TECHNOLOGY

Ecological Engineering & Environmental Technology 2022, 23(6), 128–139
https://doi.org/10.12912/27197050/152954
ISSN 2719-7050, License CC-BY 4.0

Received: 2022.07.01
Accepted: 2022.08.24
Published: 2022.09.07

Estimation of Seismic Kappa Parameter and Near-Surface Attenuation in Morocco

Abderrahim Boulanouar[1*], Himanshu Mittal[2], Abdelaali Rahmouni[3], Ahmed Zian[4], Mimoun Chourak[5], Yves Géraud[6], Mimoun Harnafi[7], Jamal Sebbani[8]

[1] Laboratory of Applied Sciences, National School of Applied Sciences, Abdelmalek Essaadi University, 03 Al Hoceima, Morocco

[2] National Center for Seismology, Ministry of Earth Sciences, New Delhi, 110003, India

[3] Laboratory of Solid State Physics, Department of Physics, Faculty of Science Dhar El Mahraz, Sidi Mohamed Ben Abdellah University, Fez 1796, Fez-Atlas, Morocco

[4] Laboratory of Engineering Sciences and Applications, National School of Applied Sciences, Abdelmalek Essaadi University, 03 Al Hoceima, Morocco

[5] Laboratory of Applied Science, National School of Applied Sciences, Mohammed First University, Oujda 60000, Morocco

[6] University of Lorraine, ENSG, UMR 7359-GeoRessources, Nancy Cedex, France

[7] Earth Science Department, Scientific Institute, Mohamed V University, P.O. Box 1014, Rabat, Morocco

[8] Mechanics and Materials Team, Faculty of Science, Mohammed V University, P.O. Box 1014, Rabat, Morocco

* Corresponding author's email: aboulanouar1@gmail.com

ABSTRACT

The goal of this study is to estimate the kappa (κ) parameter for a group of 12 broadband stations, located in different geological structures in Morocco, a country with moderate seismic activity. In this study, the kappa, κ has been obtained from the spectral analysis of the shear waves of 42 earthquakes, recorded in Morocco. Using 321 seismograms recorded in the period between 2009 and 2012 by the Picasso Project, the average κ-values have been computed from the horizontal components. For each station, the relationship between κ values and the hypocentral distance was determined. We separately investigated and studied the distance dependence of the stations located on soft soil and hard rock sites. The estimated average factor of the κ value ranges from 0.0682 for the hard sites to 0.0763 for the soft sites, with 0.072 as an average value. The lack of a significant correlation found between κ and magnitude at all stations considered in this study suggests that kappa is mainly dependent on local site characteristics. To the best of our knowledge, no studies related to kappa parameter estimation have been published for this region. The results generated in this study can be used for the seismic hazard evaluation of Morocco.

Keywords: kappa parameter, PICASSO Project, Morocco.

INTRODUCTION

In recent years, the Rif area in northern Morocco has witnessed several events (Al Hoceima earthquakes of 1994, 2004, and 2016) (Kariche et al., 2018; Boulanouar et al., 2013, Galindo-Zaldivar et al., 2018). Al Hoceima is one of the seismically active areas in northern Morocco (Boulanouar et al., 2018). Large seismic events that have been recorded and documented in seismic catalogs and research papers are evidence of this fact. This region was devastated by three severe earthquakes with moment magnitudes of more than 6 on May 26, 1994, February 24, 2004, and January 25, 2016 (Kariche et al., 2018). Any significant/*major* earthquake in the future in this

region will result in a significant loss of property and human life. To reduce the earthquake losses, seismic hazard prediction and later application to building structures, as well as the development of Morocco's current seismic code (RPS2011), are required. The kappa parameter has been identified as one of the critical parameters necessary for the evaluation of seismic hazard of a region (Yadav et al., 2018; Chandler et al., 2006).

In terms of seismic risk, areas with lower kappa values tend to have bigger ground motions than areas with higher kappa values (Douglas et al., 2010). The spectral spectrum kappa parameter κ measures the high-frequency amplitudes decay of ground motion (Biro et al., 2020). This parameter is influenced by several parameters including source parameters, velocity, propagation path, and local site characteristics (Perron et al., 2017). The kappa k parameter, which governs the decay of the acceleration spectrum for seismic recordings at high frequencies, is considered one of the most essential parameters to study the ground motion characteristics. Especially, it represents the range of attenuation energy and it is used as input for simulating strong ground motion in regions with insufficient data (Yadav et al., 2018). Several studies have been done to identify this parameter for various regions of the world (Van Houtte et al., 2011; Lai et al., 2016; Stanko et al., 2020; Mittal et al. 2021, 2022). Yadav et al. (2018) investigated the decay of the kappa parameter in the North East region of India using 598 accelerograms. They concluded that the vertical kappa values are lower than the horizontal estimations. Moreover, they observed that there was no statistically significant relationship between hypocentral distance and kappa or magnitude. Using Anderson and Hough (1984) approach for two station sites, Stanko et al. (2020) determined the kappa value for the seismic zone in Zagreb city (Croatia). According to this study, Vs30 and the predicted near-site attenuation k_0 are well correlated. In addition, the value of the k0 was lower for hard rocks and higher for soft rocks. For the northwest (NW) Himalayan region, Mittal et al. (2022) studied attenuation characteristics using 81 recorded earthquakes at 50 stations. They estimated kappa values and concluded that kappa ranges from 0.03 s to 0.095 s and is higher at the sites having sediment accumulation. Similarly, Mittal et al. (2021) estimated kappa in the Delhi region of India. Another research on kappa and its variation in distance utilizing 114 records was applied in Northwestern Iran (Samaei et al. 2016). In this work, the linear representation has a limited dependence, and they propose a clear concavity dependence in distance. The value of kappa at a great distance is observed to increase at a higher rate than at a small distance.

The main goal of this study is to estimate the kappa parameter using 12 seismic stations. The Fourier amplitude spectrum decay of acceleration in high-frequency bands for 42 local earthquakes recorded by the Picasso Project in the period between 2009 and 2012 in Morocco are analyzed in the present work. The kappa model and their R^2 indices for northern Morocco were proposed using linear regression at various seismic station locations and for different hypocentral distances. The possible dependence of the kappa (κ) on the hypocentral distance and the magnitude of the earthquake used in this study has been discussed. The effects of soft soil and hard rock sites are investigated separately. The results of this investigation will help improve our comprehension of how structures affect attenuation.

SEISMOTECTONIC SETTING

In Northwest Africa, the convergence of the African and Eurasian Plates is manifested by a complex and heterogeneous tectonic history, particularly in Northern Morocco and Western Algeria. One of the most important tectonic settings is the Gibraltar Arc system, which occurs at the western end of the Alpine orogenic belt (Morley, 1987), which includes the Alboran Sea and is surrounded by the Belt-Rif-Tell orogen. The main structural domains of this region are the Rif and tell mountains surrounding the Alboran Sea, the Moroccan and Algerian Meseta, the Atlas Mountains, and the Sahara platform (Fig. 1).

This analysis is based on two groups of stations belonging to the two structural domains described in the first paragraph: 1) The Rif and Tell Mountains domain, and 2) The Atlas Mountains domain. Regarding the Rif and Tell ranges, The estimated crustal thickness beneath the Rif cordillera ranged from a maximum of 45/50 km to a minimum of 30 km at the border with the southern portion of the Alboran Sea (De Lis Mancilla et al., 2012). This domain is distinguished by deep sedimentary, which is the result of complex tectonic movements (Chalouan et al., 2008; El Fellah et al., 2019). It consists of three primary structural domains:

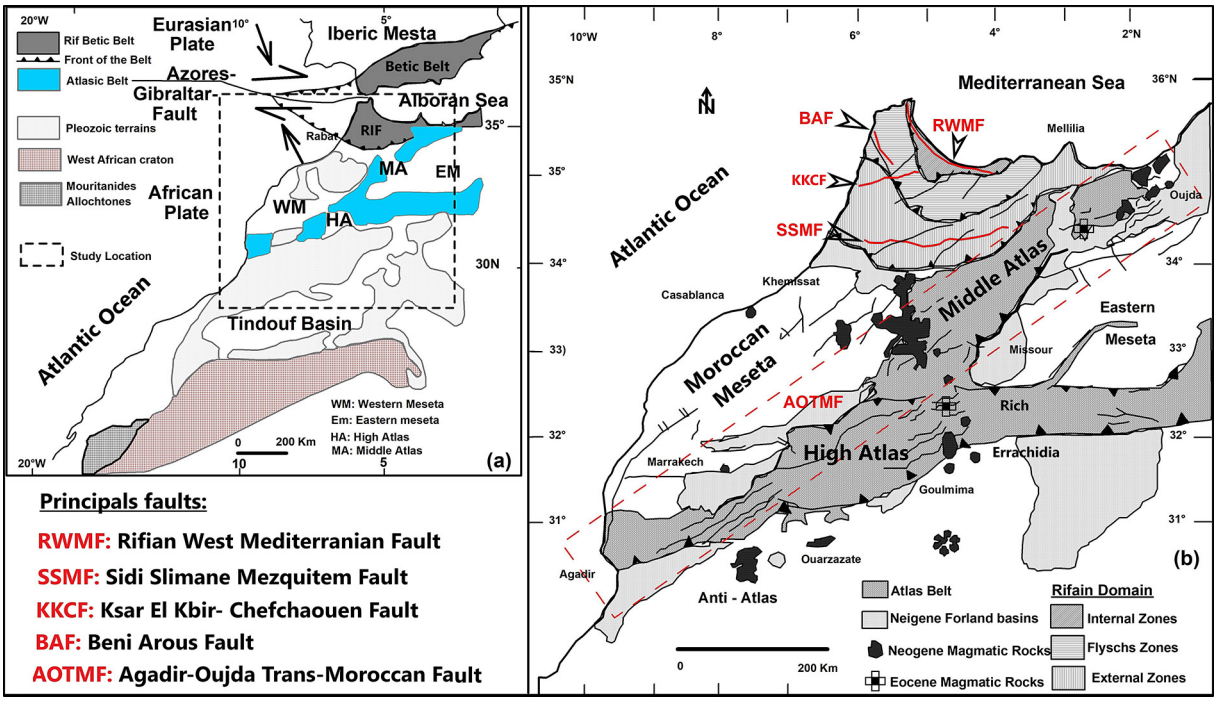

Figure 1. The main structural domains of the study area modified from (Khattach et al. 2013)

- the internal zone where these two stations (PM 04 and PM 07) are operated, consists of upper and lower plates and contains Paleozoic rocks covering Mesozoic-Cenozoic remnants (Chalouan et al., 2008);
- the complex Nappes of Flysch where PM 05 and PM 08 are deployed, are composed of two major Nappes, the Mauritanian Nappes and the massilian Nappes, which are formed in the late Mesozoic (Upper and lower cretaceous), Eocene-Oligocene and the early Miocene (Chalouan et al., 2008; De Capoa et al., 2007);
- the external zone is separated into three structural zones: intrarif (Stations: PM 11), Mesorif, and Prerif, and it is mostly composed of Cretaceous and Tertiary rocks (Andrieux, 1971; Chalouan et al, 2008).

During the 1994–2019 period, three catastrophic earthquakes occurred in the Rif region near Al Hoceima city on January 25, 2016 (Mw 6.3), February 24, 2004 (M_w 6.4), and May 26, 1994 (M_w 6.0) (Arab et al., 2020). The last earthquake did not cause as much damage as the previous two due to its offshore location and was only left on the coastline of the Rif region. While earlier earthquakes, due to their inland location, resulted in a big loss of life and caused significant damage to the infrastructure. In addition, in contrast to other areas of the world, this zone of the Iberian-African collision is characterized by moderate seismicity. As can be seen in the map of the seismicity of the Rif region (Arab et al., 2020), seismic activity is primarily concentrated within a 50-kilometer radius around Al Hoceima city, south of Nador city, and northeast of the coastline between Jebha and Tetouan city.

The Atlas Mountains are separated from the Rif Mountains by the Rharb foreland basin, where the Neogene and Quaternary sediments reach a maximum depth of eight kilometers westward. The Atlas Mountains, which are composed of Paleozoic, Mesozoic, and Tertiary rocks, are an intracontinental orogenic area situated between the Rif and Tell Mountains. They consist of the High Atlas, Middle Atlas, and Saharan Atlas in Morocco and Algeria, respectively. In contrast to the general WSW-ENE strike of the high Atlas and the Sahara Atlas, the Middle Atlas range is oriented NE-SW. Although elevations in the high Atlas reach over 4000 m, crustal thickness as revealed by available seismic data is moderate (38–39 km), which does not support crustal isostatic compensation (Fullea et al., 2007). Asthenosphere upwelling may be contributing to the uplift of the Atlas of this region (Seber et al., 1996). The Atlas Mountains are flanked by comparatively less deformed areas. The tectonic deformation in Western Maghreb is related to the oblique NW-SE convergence, creating seismic activity which is diffuse and is mostly

localized over the middle Atlas (Stations: PM21, PM 22, PM 23, PM 24, PM 25, and PM 26) and the Central High Atlas (Benouar, 1994).

SEISMIC DATA

During the 2009–2013 period, the XB network in Morocco, known as PICASSO Morocco (PM), was in operation. This investigation is based on 12 broadband stations located in different geological structures in northern Morocco. These stations are separated into two geological formations distinct. The Rif zone consists of the six stations, namely, PM04, PM05; PM07, PM08; PM011, and PM 036, whereas, the Medal Atlas includes other six stations (PM21, PM22, PM23, PM24, PM25, and PM26). Some of the stations are located on rock sites, whereas, the others are installed in soft soil environments. Table 1 shows the descriptions of the seismic sites for the Select Northern Morocco of the Picasso Project network. The stations used in this study are listed by the name of the station. About 42 events and

Table 1. Seismic site descriptions for select Northern Morocco Picasso Project network, ordered by the name of the station used in this study

Station name	Surface rock
PM04	It is a component of the complex Intra Rifain deposits: 1) The alluvial sediments of Oued Law River extend and reach approximately three to four southeast of this station. 2) The station is s located precisely between outcrop Triassic Gabbro in the Northwest and Pliocene sand and sandstone that are part of the internal zone of the Rif, especially the Ghomarids unit. 3) the Sebtids unit from the southern zone is located 4 kilometers away from the station which contains salt-gypsum deposits of the Trias.
PM05	It is part of the Flysch unit which is composed of Synclinal structures in the Northwestern and southeastern direction, formed by marls of the upper cretaceous with anormal contact of Quaternary alluvial sediments. The southwestern side is part of Numudien unit (Flysch unit) and is composed of hercynien Microgranite (lower Miocene and Oligocene) that extends 5 kilometers. The Northeastern side is part of Beni Ider uint (Flysch unit) composed of Eocene sediments deposits that extend by 5 kilometers.
PM07	Near this station, a part of the Complex Alpin epimetamorphism for the TIZGARIN unit (part of the Sebtids unit) with a salt-gypsum deposit (Triassic evaporite beds) above the thinned continental crust of the North Africa passive margin (Wildi, 1983, Chalouan et al, 2008). In the North of the station, part of the polymetamorphism with the michaschiste deposit formed the Hercynian socle.
PM08	Part of the Flysch unit (Tisiren unit), is composed of Dolerite and gabbro for the lower cretaceous and extends from the station 15 kilometers to the south. From 2 kilometers to the north of the station, a complex intra-rifain deposit with outcrop Triassic gabbro is found.
PM11	Part of the Intra-rifain unit of the external zone of the Rif. It contains Quaternary sediments (Villafranchien) that extent 8 kilometers east of the station surrounded by the big deposit of lower cretaceous divided into two units: 1) The Ketama unit in the southeast (Albian -Aptien and Neocomien) contained the Marls sediments and 2) TISIREN unit in the Northwest side which is part of the flysch unit who are composed of Cretaceous-Lower Miocene detrital rocks.
PM21	Part of the Jurassic Red Sandstone which extends about 50 kilometers in the North. The nearest plioquaternary basalts contact is 5 kilometers south of the station and after that, the Jurassic red Sandstone and a few cretaceous sediments appear in the deeper south. The serpentine and basic rock is in the west of the station.
PM22	Part of the Pleated Middle Atlas is constituted by 4 kilometers of schist-sandstone and conglomerate deposits and is surrounded by Jurassic Red Sandstone which extends 10 kilometers in the south and more than 20 kilometers in the north. The northeastern side consists of Pleistocene Lake facies within 30 kilometers. Its extension is found in the south of the area within 25 kilometers.
PM23	This station is near the last station but with the Pleistocene Lake facies and schist-sandstone + conglomerates deposit. The basaltic formation does not exceed a few hundred meters.
PM24	This station is situated in the center of the Devonian formation. To the north and northwest, there are some outcrops of Permian age rocks not exceeding a few kilometers and surrounded by Pleistocene Lake facies. The same outcrop Permian surrounded Red Sandstone and detritus facies on the Northeast side.
PM25	The station is located at the limit between Jurassic Red Sandstone from the west, Pleistocene Lake facies in the east, Cretaceous Detritus facies in the north, and quaternary sediments in the south. It is situated about 7 kilometers toward the extreme south of the chain of the High Atlas which contained basaltic rocks.
PM26	Part of the High Atlas with homogeneous basaltic rocks of the Jurassic and Lias age. It's extending from the north to the south about 78 kilometers. The station is situated in the middle this formation.
PM36	Located in the Medal Quaternary sediments extend about 10 kilometers in the south of the station which is bounded by salt-gypsum deposit (Triassic evaporite beds) in the southeastern area. The North boundary of the Quaternary sediments is 400 meters near the station and extends 17 kilometers from the station which is composed of a complex deposit of cretaceous and salt-gypsum materials.

321 seismograms with magnitudes from 1.9 to 4.8 mb are chosen to study the high-frequency attenuation parameter kappa for northern Morocco. In particular, 38 events had a magnitude greater than 3. The depth and epicentral distance of the events vary from 0 to 97.9 km, and from 9.7 to 373.58 km, respectively. Digital data were collected at a rate of 50 samples per second. An example of three-component velocity data (Vertical, north-south, and east-west component) recorded by the PM04 station of the XB network from the event of December 8, 2009 is shown in Fig. 2. The three-component waveform data for each record in our collection are baseline-corrected. Then, we manually marked arrival phases for the P and S waves. All the records are differentiated to obtain the acceleration records. Only waveforms having a signal-to-noise ratio (SNR) of 100 or above are processed and considered in the present study. The Fast Fourier transform method is used to transform the S-wave waveforms to the frequency domain. The study area with the location of the 12 seismic broadband sites and the 42 earthquakes used to determine the kappa parameter is shown in Fig. 3. Table 2 provides the lists of the epicentral information for these earthquakes. Table 3 represents the locations and duration of the seismic station used to calculate the Kappa parameter.

METHODOLOGY USED TO ESTIMATE K

Various techniques have been utilized to estimate the kappa parameter, such as the displacement kappa (Biasi and Smith, 2001), AH-Kappa (Anderson and Humphery, 1991), the acceleration Kappa approach (Biasi and Smith, 2001), and the classical kappa methodology (Anderson and Hough, 1984). Anderson and Hough (1984) presented a description of the kappa parameter k to explain the spectral shape at the high frequency for strong earthquake ground motion. They proposed that the kappa parameter has the following form:

$$A(f) = A_0 . \exp(-\pi k f), \quad f > f_E \qquad (1)$$

where: $A(f)$ indicates the acceleration spectrum and the A_0 parameter is affected by a variety of parameters such as source properties and epicentral distance.

Using the logarithms of both sides, it may be written as:

$$\ln(A(f)) = \ln A_0 - \pi k . f \qquad (2)$$

It is a linear relationship between the logarithm of acceleration spectrum and frequency. The value of the kappa parameter can be calculated by determining the slope of the following Equation:

$$k = -\lambda / \pi \qquad (3)$$

where: λ – the slope of Equation 2.

A significant relationship between kappa and distance was discovered by Anderson and Hough (1984). The equation for the linear relationship is:

$$k = k_0 + m . R \qquad (4)$$

where: k – the observable value of the kappa; k_0 – the near source attenuation or the kappa at zero distance; m – the slope of variations; R – the hypocentral distance.

In this study, the method used to estimate the kappa-value is the one proposed by Anderson and Hough (1984). Fig. 4 illustrates an example of kappa parameter estimate using spectral amplitude for the event "20091120" recorded by PM05 in the frequency range of 8–23 Hz. The best-fit lines are displayed by the solid red line.

RESULTS AND DISCUSSION

Using the method of Anderson and Hough (1984) mentioned above, the values of the kappa parameter for northern Morocco have been calculated for the horizontal components of the 321 seismograms recorded in the period between 2009 and 2012 by the Picasso Project. The stations (PM21, PM23, and PM26) had poor signals or great noise levels for several seismograms, which may affect the kappa values for these stations. Most of the Kappa values, for each station, were estimated using eight to ten events. Table 4 compares the results obtained in this study to those obtained in other parts of the world. The estimated average factor of the Kappa value ranges from 0.0682 for the hard sites to 0.0763 for the soft sites, with 0.072 as an average value. This result suggests that northern Morocco has high Kappa values when compared to other parts of the world (Yadav et al., 2018).

The mean kappa values for both of the research areas (Soft soil type and hard rocks type) are nearly identical to the kappa values obtained in Northeast India, Northwest India, and

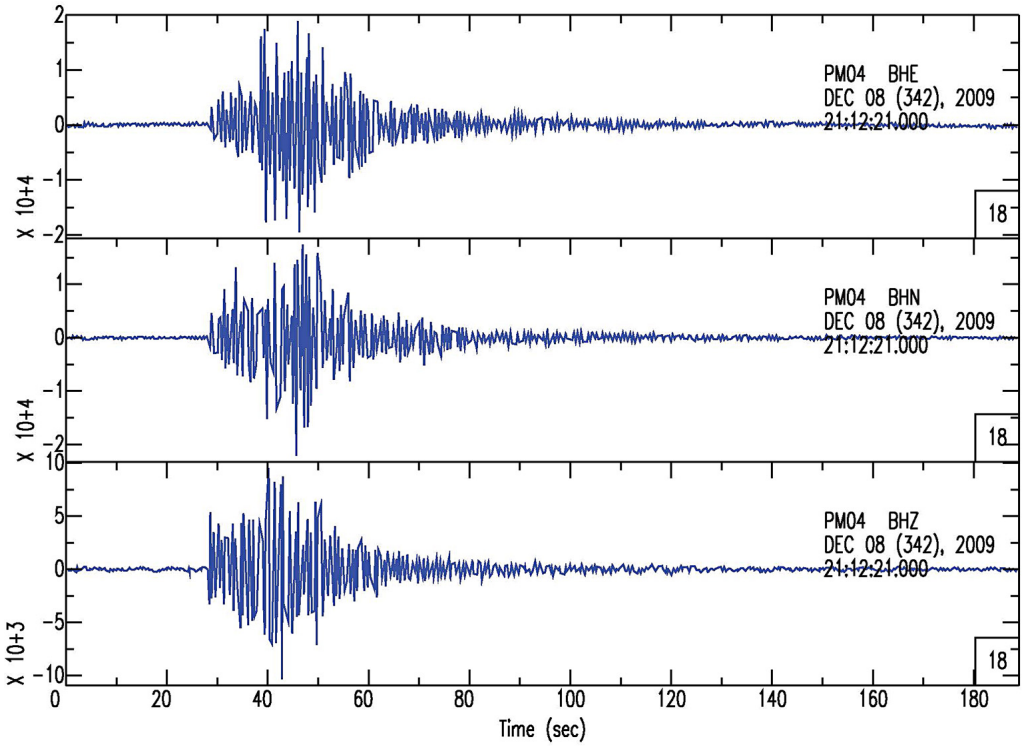

Figure 2. Example of three-component velocity records (Vertical, north–south, east–west component) recorded by PM04 of the XB network from the event on 08 December 2009. BHZ is the vertical component; BHN is the North-South component; BHE is the East-West component

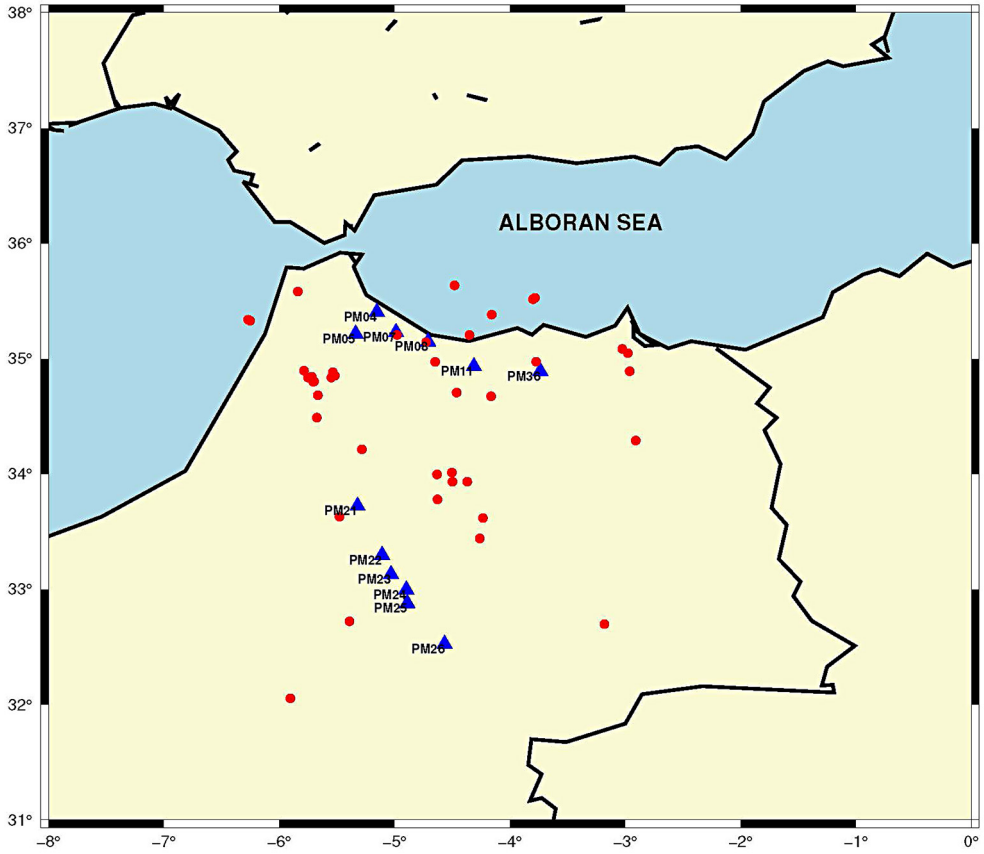

Figure 3. Location of earthquakes in the red circle and recording stations in the blue triangle icon used in the present study (Wessel and Smith 2004)

Table 2. List of earthquakes used for the estimation of kappa parameter, *k*

ID event	Depth	Magnitude	Latitude	Longitude
200911201915	25.7	3.8	34.8506	-5.5166
20091208211238	14.8	3	34.834	-5.5473
20100214221434	27.1	4.2	34.882	-5.5342
201002070934	7.1	3.7	34.894	-5.7842
201001190158	10	3.5	34.704	-4.4617
20100121165707	12.9	4.5	34.7985	-5.7031
201002070320	30	3.1	34.8414	-5.7165
20100213050309	10	4	34.8347	-5.7499
201003071635	73.8	3.6	35.203	-4.9779
201004220123	42.2	4.8	35.3272	-6.2519
201004131138	35.9	3.8	34.6806	-5.6645
20100219041311	10	4.3	33.4391	-4.2612
201001250235	60	3.4	35.58	-5.8377
20100123002907	10	3.7	32.6964	-3.1803
201003230531	13.8	3.7	33.6287	-5.4764
201003150013	24	3.7	33.9941	-4.6317
20100219041309	10	3.5	33.616	-4.233
201003120851	24	3.8	34.0097	-4.5022
201003271421	0	3.8	33.7785	-4.6277
201003171651	26.5	3.8	35.203	-4.3495
201003140537	20	3.0	33.9313	-4.3693
201003120317	24	3.6	33.9312	-4.4972
20110210212542	11.3	4	34.2882	-2.9082
201102140602	10.9	4.5	32.0523	-5.9026
201102150115	28.4	3.5	34.972	-3.7713
201102180110	23.8	4.2	35.6338	-4.4791
201105010450	6.3	4.3	32.7206	-5.3896
201107180226	10	Ml=2.3	34.6729	-4.1626
201109292044	35	Ml=3.2	34.9709	-4.6479
20110301102626	97.9	3.7	35.1406	-4.7261
20120704074416	19.8	4	34.8894	-2.9617
20120710041952	19	3.8	34.2113	-5.2821
201009050333	14.7	3.3	35.0823	-3.0246
201009110357	15.1	3.0	35.0467	-2.9775
20100422014248	53.9	3.2	35.3366	-6.2688
201202180028	29.6	4.2	34.4874	-5.6734
201207040744	19.8	4.0	34.8894	-2.9617
201012141745	8.9	3.6	35.3796	-4.1563
201102102125	11.3	4.0	34.2882	-2.9082
20101016035249	17.6	2.9	35.5132	-3.7984
20101016035251	10	1.9=Ml	35.5256	-3.7817
20100414152119	10	4.1	34.8001	-5.6973

Saint-Louis, USA (Table 4). Low values of the mean of the kappa parameter are found in several regions such as Switzerland by 0.015, the Western Alps by 0.0125, and mainland French by 0.04–0.06. The low kappa value indicates that the local geology has very little impact on high-frequency attenuation (Rinne, 2021). Due to the high kappa value obtained in this study,

Table 3. Locations and duration of the 13 seismic stations used in this study

Network	Station	Latitude	Longitude	Elevation	Start time	End time
XB	PM04	35.402599	-5.1525	111.0	2009-02-11T00:00:00	2012-10-31T23:59:00
XB	PM05	35.213402	-5.3368	510.0	2009-11-01T00:00:00	2012-10-30T23:59:00
XB	PM07	35.227501	-4.9863	711.0	2009-11-02T00:00:00	2012-10-31T23:59:00
XB	PM08	35.144798	-4.7082	253.0	2009-11-02T00:00:00	2012-10-31T23:59:00
XB	PM11	34.930801	-4.3119	1004.0	2009-11-03T00:00:00	2012-10-31T23:59:00
XB	PM21	33.720501	-5.3197	1013.0	2009-10-28T00:00:00	2013-05-27T23:59:00
XB	PM22	33.294701	-5.1071	1945.0	2009-10-22T00:00:00	2009-10-29T00:00:00
XB	PM22	33.294701	-5.1071	1945.0	2009-10-29T00:00:00	2011-03-09T11:30:00
XB	PM23	33.127998	-5.0300	1990.0	2009-10-22T00:00:00	2013-05-27T23:59:00
XB	PM24	32.9953	-4.8979	1599.0	2009-10-22T00:00:00	2013-05-27T23:59:00
XB	PM25	32.875702	-4.8880	1417.0	2009-10-20T00:00:00	2013-05-27T23:59:00
XB	PM26	32.524502	-4.5659	1840.0	2009-10-20T00:00:00	2013-05-26T23:59:00
XB	PM36	34.8894	-3.7359	776.0	2010-10-19T00:00:00	2012-10-30T23:59:00

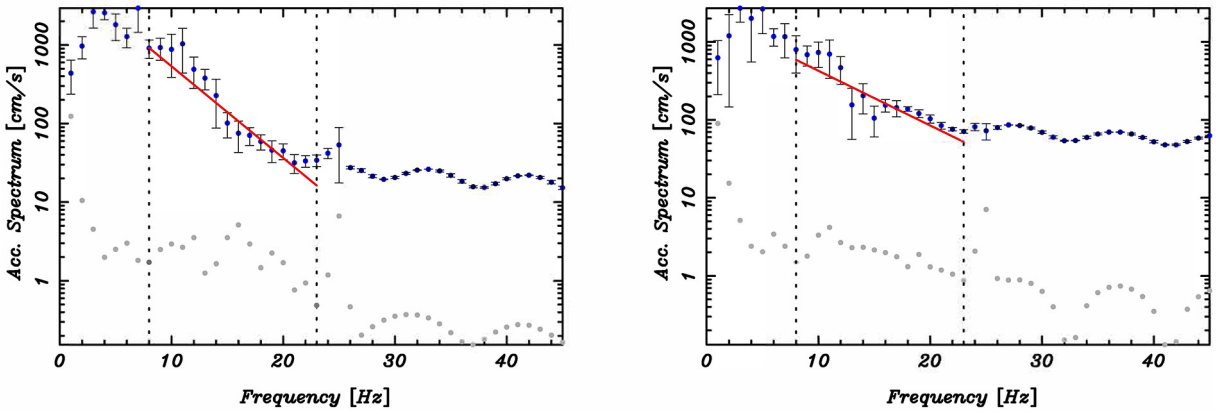

Figure 4. Example of kappa parameter estimation using spectral amplitude in the frequency band of 8-23Hz for the event «20091120» which was recorded by PM05. The solid red line shows the best-fitted lines

Table 4. Compares results obtained from this study with those from other parts of the world

Region	Mean Kappa value	Reference
Switzerland	0.015	Bay et al. 2003
Switzerland	0.0125	Bay et al. 2005
Western Alps	0.012	Morasca et al.2006
mainland France	0.04 for rock sites	Douglas et al. 2010
Northeast India	0.0637 for firm ground type of site	Awasthi et al. 2010
Northeast India	0.0756 for soft rock type	Awasthi et al. 2010
Northwest India	0.03–0.095 for various sites	Mittal et al. (2022)
Delhi region, India	0.0118–0.0537 for various sites	Mittal et al. (2021)
Saint-Louis	0.007	Hermann and Akinci (1999)
Memphis	0.063	Hermann and Akinci (1999)
Greece	0.060	Margaris et al. (1998)

the local sites of the seismic stations have a significant influence on the high-frequency attenuation. Figure 5 shows the existing correlation between the kappa parameter and the hypocentral distance and Figure 6 illustrates the dependency of the kappa parameter on the hypocentral distance for all 12 seismic stations used in this study. The distance-dependency of the kappa laws for

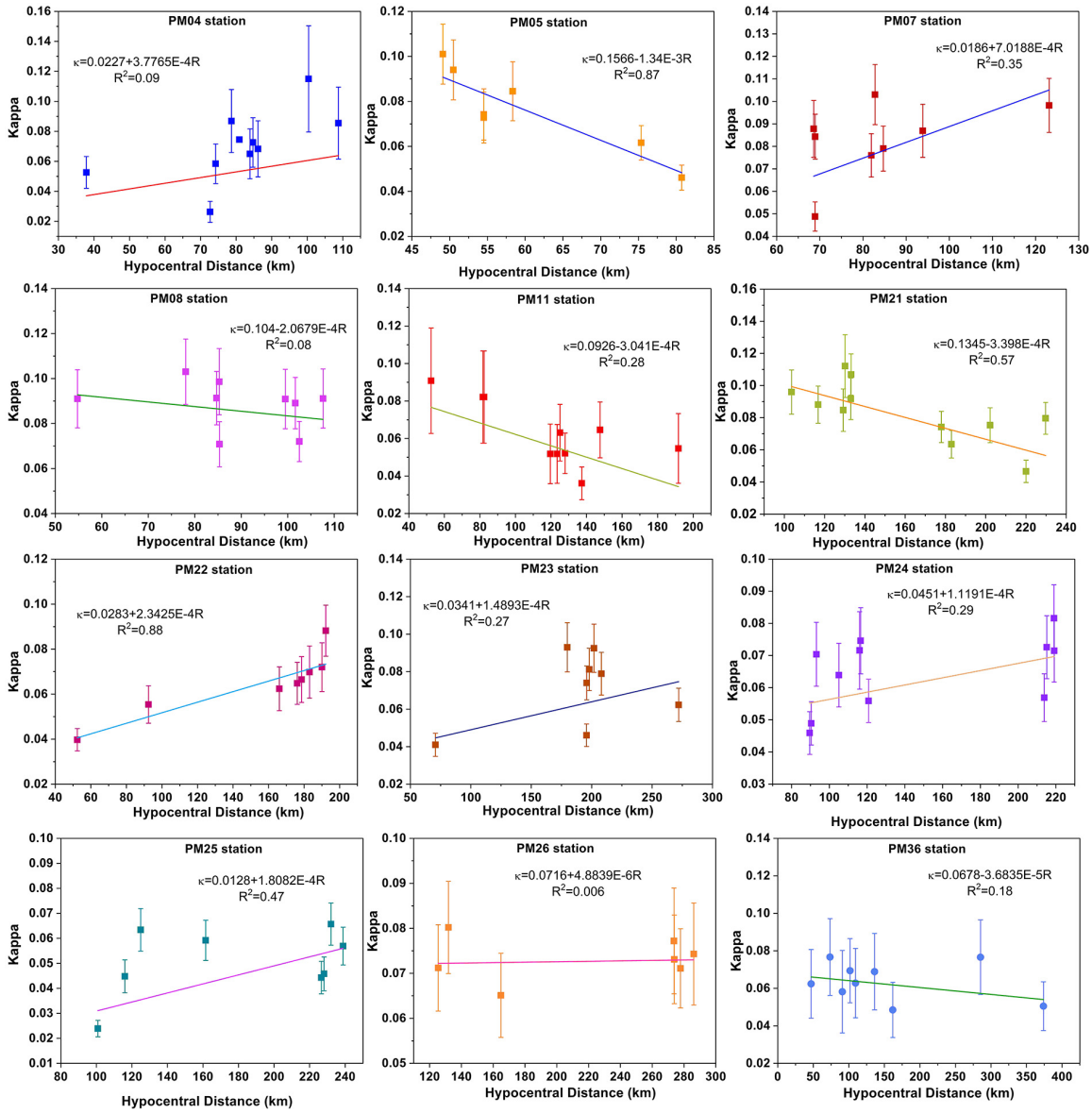

Figure 5. Correlation of the kappa parameter for each seismic station site with the hypocentral distance and their error for northern Morocco

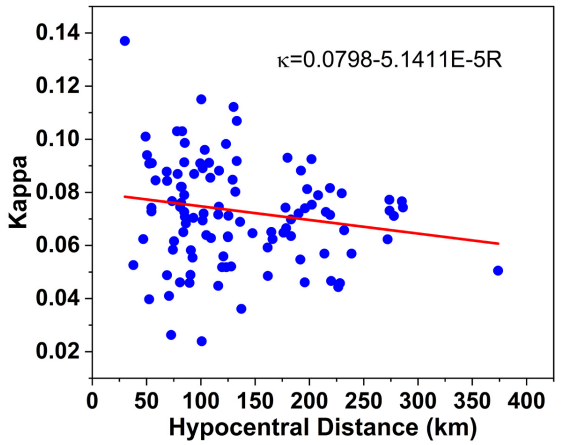

Figure 6. Dependency of kappa parameter on the hypocentral distance for all 12 seismic stations used in this study

each pair station-event is, using linear regression, shown at the top of each plot accompanied by the dependency index R-square. A highly significant correlation between the Kappa parameter and the hypocentral distance was observed for some station sites such as PM05, PM21, and PM22, and a low correlation was observed in others. The reason could be the low number of data per station or high seismic noise recorded for some stations or both. Also, the kappa value is sensitive to the data selection criteria and the methodology choice (Palmer and Atkinson, 2020). In Indian Himalayan region, Yadav et al. (2018) and Mittal et al. (2021, 2022) found that the distance dependence is not significant. Additionally, they observed that

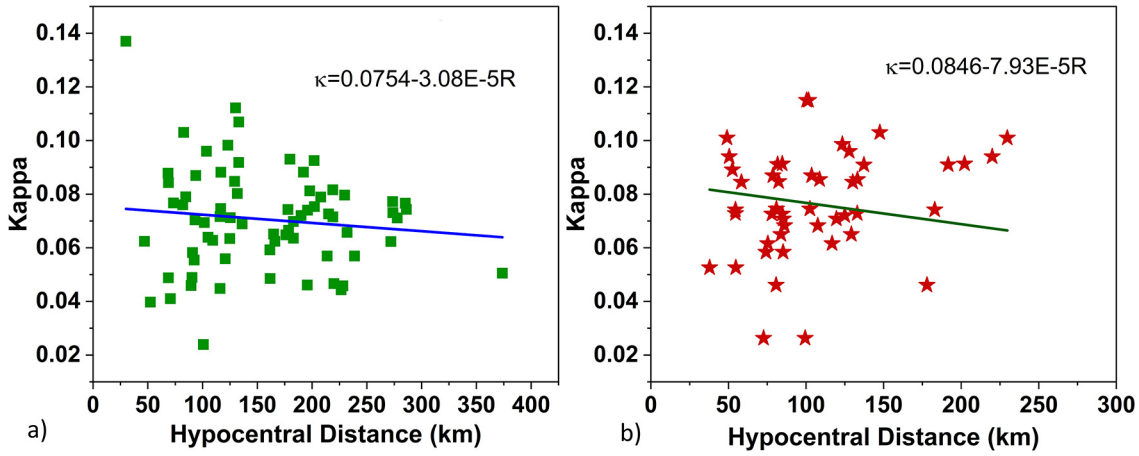

Figure 7. Distance-dependence of kappa for a) hard rock sites and b) soft soil sites

there is no clear distance dependence for both the horizontal and the vertical components. The near-source parameter, κ_0, obtained from the station dependence at zero distance, indicates the site attenuation immediately under the station site (Hough and Anderson, 1988). It is a unique property of the seismic site (Awasthi et al., 2010). Once the dependency equation of the kappa parameter for each event-station pair has been determined, the near-surface attenuation parameter k_0 is derived using equation (4).

Figure 7 illustrates the distance dependence of kappa for hard rock sites and soft soil sites. For hard rock sites, the linear fit relation is k = 0.0754-3E-05R and for soft rock type sites, k = 0.0847-8E-05R. k_0 is 0.0754 for hard rock type sites and 0.0847 for soft rock sites. This indicates that the value of near-surface attenuation for soft rock stations has a higher value than those of hard rock type sites. This result is consistent with the experimental research conducted by Yadav et al. (2018) in North East India. In France, Douglas et al. (2010) observed that kappa is affected by the local geology proprieties and hypocentral distance. They have found κ_0 = 0.0270 for soft soil rocks and κ_0 = 0.0207 for hard rocks. For Guerrero, Mexico, Humphrey and Anderson (1992) discovered no relationship between the kappa parameter and site geology. In the Kachchh region of Gujarat, India, Kumar et al. (2018) found that κ_0 = 0.016 for hard rock sites and κ_0 = 0.0201 for soft rock sites. Using data from the ANZA Seismic Network, Kilb et al. (2012) found κ_0 = 0.036 for soil soft rock sites and κ_0 = 0.030 for hard rock sites in Southern California. Chang et al. (2019) calculated the near-surface attenuation parameter for the Taiwan region and found that its values vary from 0.032 to 0.097 at the surface and from 0.012 to 0.078 in the borehole.

CONCLUSIONS

Using the Anderson and Hough technique (1984), we have calculated the kappa proprieties from the horizontal components for the region of northern Morocco through the spectral decay amplitude at high frequencies. The estimated average factor of the Kappa value ranges from 0.0682 for the hard sites to 0.0763 for the soft sites, with 0.072 as an average value. According to this finding, northern Morocco has higher Kappa values than other regions of the world. The linear fit relation for hard rock sites is k = 0.0754-3E-05R and for soft rock sites is k = 0.0847-8E-05R. It means that the near-surface attenuation, k_0, is 0.0754 for hard rock sites and 0.0847 for soft rock sites. It implies that the near-surface attenuation for soft rock stations is higher than the hard rock type sites. The average kappa values for both research areas (Soft rock type and hard rock type) are very similar to those observed in Northeast India and Saint-Louis, USA. For some station sites, including PM05, PM21, and PM22, a highly significant correlation between the Kappa parameter and the hypocentral distance was seen, although a poor correlation was seen in other cases. These results can be used for the seismic hazard evaluation of Morocco.

Acknowledgments

All seismic data used in this study, belonging to the Program to Investigate Convective Alboran Sea System Overturn, were retrieved from the

Incorporated Research Institutions for Seismology (IRIS) (ORFEUS Data Center) at the website: http://www.fdsn.org/networks/detail/XB_2009. All data retrieved from this project are openly available (Last accessed in August 2022). The author Himanshu Mittal is thankful to Director, National Centre for Seismology, Ministry of Earth Sciences, India for his support to participate in the present work. Figure 3 is created with the GMT software (Wessel and Smith 2004).

REFERENCES

1. Anderson J.G., Hough S.E. 1984. A model for the shape of the Fourier amplitude spectrum of acceleration at high frequencies. Bulletin of the Seismological Society of America, 74, 1969–1993.
2. Anderson J.G., Humphrey J. 1991. A least-squares method for objective determination of earthquake source parameters. Seismological Research Letters, 62, 201–209.
3. Andrieux J., Fontbote J.M., Mattauer M. 1971. Sur un modèle explicatif de l'Arc de Gibraltar. Earth and Planetary Science Letters, 12(2), 191–198.
4. Arab O., Azguet R., Ouchen I., El Fellah Y., Harnafi M., Sebbani, et al. 2020. Attenuation of seismic coda waves in the Rif area, northern Morocco. Journal of African Earth Sciences, 165, 103815.
5. Awasthi D.K., Shende V.J., Gupta I.D. 2010. Estimation of κ factor for two types of sites in northeast India. Indian Geotechnical Conference, 16–18.
6. Bay F., Fäh D., Malagnini L., Giardini D. 2003. Spectral shear-wave ground-motion scaling in Switzerland. Bulletin of the Seismological Society of America, 93(1), 414–429.
7. Bay F., Wiemer S., Fäh D., Giardini D. 2005. Predictive ground motion scaling in Switzerland: best estimates and uncertainties. Journal of Seismology, 9(2), 223–240.
8. Benouar D. 1994. Materials for the investigation of the seismicity of Algeria and adjacent regions during the twentieth century. Annali de geofisica, 37(4), 609–835.
9. Biasi G.P., Smith K.D. 2001. Site effects for seismic monitoring stations in the vicinity of Yucca Mountain, Nevada. A report prepared for the US DOE/University and Community College System of Nevada (UCCSN) Cooperative Agreement. MOL20011204.0045. Nevada (US).
10. Biro Y., Siyahi B., Akbas B. 2020. The spectral decay parameter κ (kappa) for hard rock strong ground motion stations in Turkey. 17th World Conference on Earthquake Engineering, 3–18.
11. Boulanouar A., El Moudnib L., Harnafi M., Cherkaoui T. E., Rahmouni A., Boukalouch M., Sebbani J. 2013. Spatial variation of coda wave attenuation using aftershocks of the Al Hoceima earthquake of 24 February, 2004, Morocco. Natural Science, 5(8), 72.
12. Boulanouar A., Moudnib L.E., Padhy S., Harnafi M., Villaseñor A., et al. 2018. Estimation of coda wave attenuation in Northern Morocco. Pure and Applied Geophysics, 175(3), 883–897.
13. Chalouan A., Michard A., Kadiri K., Negro F., Lamotte D., Soto J.I., et al. 2008. Continental evolution: the geology of Morocco. Springer Berlin, Heidelberg.
14. Chandler A.M., Lam N.T., Tsang H.H. 2006. Near surface attenuation modelling based on rock shear wave velocity profile. Soil Dynamics and Earthquake Engineering, 26, 1004–1014.
15. Chang S.C., Wen K.L., Huang M.W., Kuo C.H., Lin, C. M., et al. 2019. The high-frequency decay parameter (Kappa) in Taiwan. Pure and Applied Geophysics, 176(11), 4861–4879.
16. De Capoa P., Di Staso A., Perrone V., Zaghloul M.N. 2007. The age of the foredeep sedimentation in the Betic–Rifian Mauretanian units: a major constraint for the reconstruction of the tectonic evolution of the Gibraltar Arc. Comptes Rendus Geoscience, 339(2), 161–170.
17. Douglas J., Gehl P., Bonilla L.F., Gélis C. 2010. A κ model for mainland France. Pure and applied geophysics, 167(11), 1303–1315.
18. De Lis Mancilla F., Stich D., Morales J., Julià J., Diaz J., et al. 2012. Crustal thickness variations in northern Morocco. Journal of Geophysical Research: Solid Earth, 117(B2).
19. El Fellah Y., Bouskri G., Harnafi M., Abd El A.E.A.K., Timoulali Y., et al. 2019. Tracking regional heterogeneities through seismic ambient noise constrains: What Rayleigh wave tomography can tell about deep structures in northern Morocco. Journal of African Earth Sciences, 160, 103615.
20. Fullea J., Fernandez M., Zeyen H., Vergés J. 2007. A rapid method to map the crustal and lithospheric thickness using elevation, geoid anomaly and thermal analysis. Application to the Gibraltar Arc System, Atlas Mountains and adjacent zones. Tectonophysics, 430(1–4), 97–117.
21. Galindo-Zaldivar J., Ercilla G., Estrada F. Catalán, M., d'Acremont E., et al. 2018. Imaging the growth of recent faults: The case of 2016–2017 seismic sequence sea bottom deformation in the Alboran Sea (Western Mediterranean). Tectonics, 37(8), 2513–2530.
22. Herrmann R., Akinci A. 1999. Mid-America ground motion models, http://www.eas.slu.edu/People/RBHerrmann/MAEC/maecgnd.html
23. Hough E., Anderson J.G. 1988. High-frequency spectra observed at Anza, California: Implications

for Q structure. Bulletin of the Seismological Society of America, 78(2), 692–707.

24. Humphrey J.R., Anderson J.G. 1992. Shear wave attenuation and site response in Guerrero Mexico. Bulletin of the Seismological Society of America, 81, 1622–1645.
25. Kariche J., Meghraoui M., Timoulali Y., Cetin E., Toussaint R. 2018. The Al Hoceima earthquake sequence of 1994, 2004 and 2016: Stress transfer and poroelasticity in the Rif and Alboran Sea region. Geophysical Journal International, 212(1), 42–53.
26. Khattach D., Houari M.R., Corchete V., Chourak M., El Gout R., Ghazala H. 2013. Main crustal discontinuities of Morocco derived from gravity data. Journal of Geodynamics, 68, 37–48.
27. Kilb D., Biasi G., Anderson J., Brune J., Peng Z., Vernon F.L. 2012. A comparison of spectral parameter kappa from small and moderate earthquakes using southern California ANZA seismic network data. Bulletin of the Seismological Society of America, 102(1), 284–300.
28. Kumar S., Kumar D., Rastogi B.K., Singh A.P. 2018. Kappa (κ) model for Kachchh region of Western India. Geomatics, Natural Hazards and Risk, 9(1), 442–455.
29. Lai T.S., Mittal H., Chao W.A., Wu Y.M. 2016. A study on Kappa value in Taiwan using borehole and surface seismic array. Bulletin of the Seismological Society of America, 106(4), 1509–1517.
30. Margaris B.N., Boore D.M. 1998. Determination of Δσ and κ0 from response spectra of large earthquakes in Greece. Bulletin of the Seismological Society of America, 88(1), 170–182.
31. Mittal H., Sharma B., Chao W.A., Wu Y.M., Lin T.L., Chingtham P. 2022. A comprehensive analysis of attenuation characteristics using strong ground motion records for the Central Seismic Gap Himalayan Region, India. Journal of Earthquake Engineering, 26(5), 2599–2624.
32. Mittal H., Sharma B., Sandhu M., Kumar D. 2021. Spatial distribution of high-frequency spectral decay factor kappa (κ) for Delhi, India. Acta Geophysica, 69(6), 2113–2127.
33. Morley K. 1987. Origin of major cross element zone: Morocco Rif. Geology, 15, 761–764.
34. Palmer S.M., Atkinson G.M. 2020. The high-frequency decay slope of spectra (kappa) for M≥ 3.5 earthquakes on rock sites in Eastern and Western Canada. Bulletin of the Seismological Society of America, 110(2), 471–488.
35. Perron V., Hollender F., Bard P.Y., Gélis C., Guyonnet-Benaize C., Hernandez B., Ktenidou O.J. 2017. Robustness of Kappa (κ) Measurement in Low-to-Moderate Seismicity Areas: Insight from a Site-Specific Study in Provence, France. Bulletin of the Seismological Society of America, 107(5), 2272–2292.
36. Rinne L. 2021. Seismic wave attenuation and the spectral decay parameter κ (kappa) in crystalline bedrock at Olkiluoto, SW Finland. Master's thesis, University of Helsink, Finland.
37. Samaei M., Miyajima M., Yazdani A., Jaafari F. 2016. High Frequency Decay Parameter (Kappa) for Ahar–Varzaghan Double Earthquakes, Iran (MW 6.5 and 6.3). Journal of Earthquake and Tsunami, 10(2), 1640006.
38. Seber D., Barazangi M., Ibenbrahim A., Demnati A. 1996. Geophysical evidence for lithospheric delamination beneath the Alboran Sea and Rif–Betic mountains. Nature, 379(6568), 785–790.
39. Stanko D., Markušić S., Korbar T., Ivančić J. 2020. Estimation of the high-frequency attenuation parameter kappa for the Zagreb (Croatia) seismic stations. Applied Sciences, 10(24), 8974.
40. Van Houtte C., Drouet S., Cotton F. 2011. Analysis of the origins of κ (kappa) to compute hard rock to rock adjustment factors for GMPEs. Bulletin of the Seismological Society of America, 101(6), 2926–2941.
41. Wessel P., Smith W.H.F. 2004. Generic Mapping Tools Graphics.
42. Wildi W. 1983. La chaîne tello-rifaine (Algérie, Maroc, Tunisie): structure, stratigraphie et évolution du Trias au Miocène. Revue de géographie physique et de géologie dynamique, 24(3), 201–297.
43. Yadav R., Kumar D., Chopra S. 2018. The high frequency decay parameter κ (kappa) in the region of North East India. Open Journal of Earthquake Research 7, 141–159.